

The effective electroweak mixing angle $\sin^2 \theta_{\text{eff}}$ with two-loop bosonic contributions

W. HOLLIK¹, U. MEIER¹ and S. UCCIRATI²

¹ Max-Planck-Institut für Physik
(Werner-Heisenberg-Institut)
D-80805 München, Germany

² Dip. di Fisica Teorica, Università di Torino,
INFN Sezione di Torino
10125 Torino, Italy

Abstract

We present the results for the full electroweak two-loop bosonic contributions to the effective leptonic mixing angle of the Z boson, $\sin^2 \theta_{\text{eff}}$, in the Standard Model. A method applied to extract collinear divergences from two-loop vertex-functions is described. Comparisons of our results with those from a recent previous calculation show complete agreement.

1 Introduction

Measurements of the various asymmetries of the Z resonance have determined the effective leptonic mixing angle $\sin^2\theta_{\text{eff}}$ with high accuracy. The current experimental value is 0.23153 ± 0.00016 [1]; a linear electron-positron collider with GigaZ capabilities could even reach an accuracy of 1.3×10^{-5} [2, 3]. Comparison with the theoretical prediction of the Standard Model yields stringent bounds on the Higgs-boson mass M_H . The importance and precision of $\sin^2\theta_{\text{eff}}$ requires sufficient control on the theoretical accuracy of the prediction by providing adequate higher-order calculations.

$\sin^2\theta_{\text{eff}}$ is determined from the ratio of the dressed vector and axial vector couplings $g_{V,A}$ of the Z boson to leptons [4],

$$\sin^2\theta_{\text{eff}} = \frac{1}{4} \left(1 - \text{Re} \frac{g_V}{g_A} \right). \quad (1)$$

In the on-shell renormalization scheme, it is related to the vector-boson mass ratio or, equivalently, to the on-shell quantity $s_W^2 = 1 - M_W^2/M_Z^2$ via

$$\sin^2\theta_{\text{eff}} = \kappa s_W^2, \quad \kappa = 1 + \Delta\kappa, \quad (2)$$

involving the κ factor, which is unity at the tree level and accommodates the higher-order contributions in $\Delta\kappa$. M_W can be related to the precisely known Fermi constant G_μ via the relation

$$M_W^2 \left(1 - \frac{M_W^2}{M_Z^2} \right) = \frac{\pi\alpha}{\sqrt{2}G_F} (1 + \Delta r), \quad (3)$$

where Δr summarizes the higher-order contributions. Beyond the one-loop order, the universal QCD corrections [5, 6], the complete electroweak fermionic [7] and bosonic [8] two-loop corrections, as well as leading higher-order contributions via the ρ -parameter [9, 10] and the S -parameter [11] are known for the Standard Model.

The universal higher-order terms to the self-energies from QCD and through the ρ - and S -parameter enter also the quantity $\Delta\kappa$ in (2). The fermionic electroweak two-loop corrections (involving at least one closed fermion loop) have been established [12, 13]; the M_H -dependence of the bosonic corrections to $\Delta\kappa$ was given in [14], and only recently a complete calculation of the bosonic contributions was reported [15].

In this paper we complete our result for the bosonic two-loop contributions by accomplishing the M_H -independent part of $\Delta\kappa$, which was missing in [14]. Together with our result from [14], this yields an independent result for the complete bosonic two-loop corrections for $\sin^2\theta_{\text{eff}}$, based on different methods.

2 Computational strategy

Expanding the dressed couplings in (1) according to $g_{V,A} = g_{V,A}^{(0)} \left(1 + g_{V,A}^{(1)} + g_{V,A}^{(2)} + \dots \right)$ in powers of α , the $O(\alpha^2)$ contribution to $\sin^2\theta_{\text{eff}}$ in the loop expansion

$$\sin^2\theta_{\text{eff}} = \sin^2\theta_{\text{eff}}^{(0)} + \sin^2\theta_{\text{eff}}^{(1)} + \sin^2\theta_{\text{eff}}^{(2)} + \mathcal{O}(\alpha^3) \quad (4)$$

is obtained,

$$\sin^2\theta_{\text{eff}}^{(2)} = -\frac{g_V^{(0)}}{4g_A^{(0)}} \text{Re} \left(g_V^{(2)} - g_A^{(2)} + g_A^{(1)} \left(g_A^{(1)} - g_V^{(1)} \right) \right). \quad (5)$$

Hence, besides two-loop diagrams, also products of one-loop contributions have to be taken into account. They play an important role in the cancellation of IR-divergences (see section 3). But the major task consists in the calculation of irreducible two-loop $Z\ell\ell$ -vertex diagrams ($\ell = e$, to be precise). The Z -boson couplings in (1) appear in the renormalized $Z\ell\ell$ vertex for on-shell Z bosons; for the two-loop contributions entering the expression (5) we need the renormalized two-loop vertex

$$\hat{\Gamma}_\mu^{Z\ell\ell(2)}(M_Z^2) = \gamma_\mu \left(g_V^{(2)} - g_A^{(2)} \gamma_5 \right). \quad (6)$$

As done in [13, 14] we split the renormalized vertex into two UV -finite pieces,

$$\begin{aligned} \hat{\Gamma}_\mu^{Z\ell\ell(2)}(M_Z^2) &= \Gamma_\mu^{Z\ell\ell(2)}(M_Z^2) + \Gamma_\mu^{CT} \\ &= \left[\Gamma_\mu^{Z\ell\ell(2)}(0) + \Gamma_\mu^{CT} \right] + \left[\Gamma_\mu^{Z\ell\ell(2)}(M_Z^2) - \Gamma_\mu^{Z\ell\ell(2)}(0) \right]. \end{aligned} \quad (7)$$

$\Gamma_\mu^{Z\ell\ell(2)}(M_Z^2)$ denotes the corresponding unrenormalized $Z\ell\ell$ vertex for on-shell leptons and momentum transfer $P^2 = M_Z^2$, and Γ_μ^{CT} is the two-loop counter term. Details on the renormalization are given in [13], where the expressions are general and comprise also the bosonic two-loop contributions.

The first term in (7) can be computed as in the fermionic case, which means generating Feynman diagrams with the help of *FeynArts* [16] and applying *TwoCalc* [17] to reduce the amplitudes to standard integrals. The resulting vacuum integrals are calculated using analytic results [18, 19], whereas the two-loop self-energies with non-vanishing external momenta, which appear in the counter terms, are calculated with the help of one-dimensional integral representations [20] or the methods described in [21].

The IR -finite contributions to the second term in (7) can be calculated in analogy to the M_H -dependent part of the bosonic corrections [14]. This means that vertex corrections are computed applying the methods from [21] together with further improvements in order to increase the numerical stability. Non-planar diagrams are calculated using the method described in [14], and diagrams with self-energy insertions are computed using dispersion relations as described in [13].

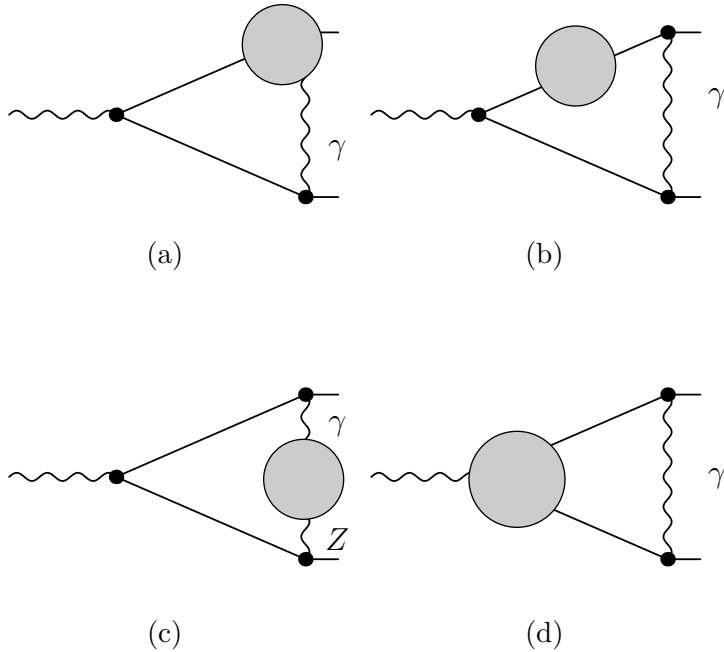


Figure 1: Diagrams with IR-divergences

3 Treatment of IR- and collinear divergences

As a new feature compared to the M_H -dependent subset of the bosonic corrections, diagrams with internal photons appear that can be IR-divergent. These divergences, however, cancel in the complete result rendering $\sin^2\theta_{\text{eff}}$ as a IR-finite quantity.

The IR-divergent diagrams are shown in Fig. 1. The grey circles represent one-loop insertions. In order to verify the cancellation of these divergences, we have used the methods described in [22]. These methods allow to extract all appearing IR-divergences in terms of IR-divergent one-loop integrals. After this extraction the cancellation of these integrals can be checked analytically. The cancellation occurs between the various two-loop diagrams within the set of Fig. 1(a)-(c), and between the two-loop diagrams of Fig. 1(d) and the product of one-loop diagrams occurring in (5). This is shown schematically in Fig. 2.

Moreover, collinear divergences appear. In order to regularize them we have kept the electron mass m_e finite where necessary. In addition we have expanded the resulting expressions in m_e , so that the divergent behavior shows up as terms proportional to $\ln^2(m_e^2)$ and $\ln(m_e^2)$. Afterwards it was checked analytically that the terms proportional to $\ln^2(m_e^2)$ cancel, whereas the cancellation of the $\ln(m_e^2)$ -terms was checked numerically. Our methods to extract these logarithms are explained in the following section 4 by means of the two non-planar diagrams shown in Fig. 3.

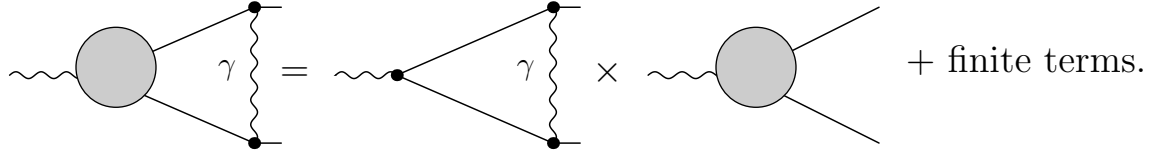


Figure 2: Compensation of IR-divergences

4 Extraction of collinear divergences

Collinear divergences can show up in massive diagrams which do not contain any soft divergences, or they can overlap with soft divergences. In both cases we have managed to extract explicitly the coefficients of the logarithms in m_e^2 (which is the natural regulator for these divergences) and the constant term. For overlapping divergences we have used the results of [22], while for the other ones we have used a subtraction method in parametric space. In order to explain it we consider the two collinear configurations of the non-planar diagrams in Fig. 3, which arise in the computation.

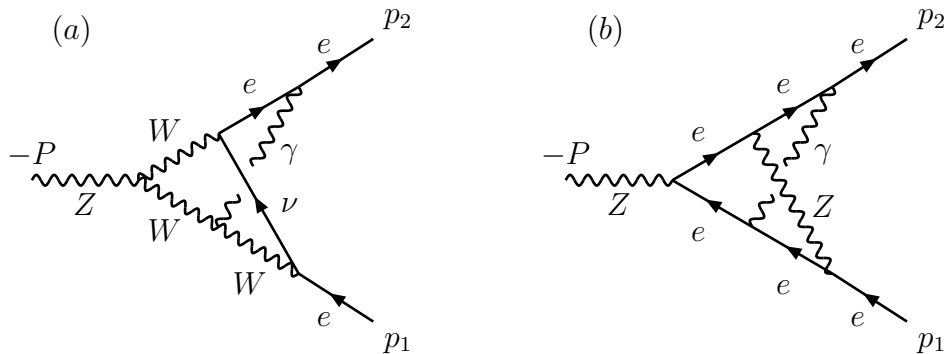


Figure 3: Examples for collinearly divergent diagrams. All momenta are incoming, and $P = p_1 + p_2$.

In momentum space the generic diagram contains the following scalar and tensor integrals,

$$V_{222}^{(1,\mu,\mu\nu,\mu\nu\rho)} = -\frac{1}{\pi^4} \int d^4 q_1 \int d^4 q_2 \frac{(1, q_1^\mu, q_1^\mu q_1^\nu, q_1^\mu q_1^\nu q_1^\rho)}{[1][2][3][4][5][6]}, \quad (8)$$

$$\begin{aligned} [1] &= q_1^2 - m_1^2, & [2] &= (q_1 - p_2)^2 - m_2^2, & [3] &= (q_1 - q_2 + p_1)^2 - m_3^2, \\ [4] &= (q_1 - q_2 - p_2)^2 - m_4^2, & [5] &= q_2^2 - m_5^2, & [6] &= (q_2 - p_1)^2 - m_6^2. \end{aligned}$$

Following the discussion given in [21], we first combine the propagators [1] and [2] with a Feynman-parameter z_1 , the propagators [3] and [4] with a Feynman-parameter z_2 , and the propagators [5] and [6] with a Feynman-parameter z_3 . Then we combine the q_1 and $q_1 - q_2$ propagators with a parameter x . After the q_1 -integration we combine the residual propagators with a parameter y and carry out the q_2 integration. For the scalar integral $V_{222}^{(1)}$, the resulting expression reads (we have changed $x \rightarrow 1 - x$ with respect to [21]):

$$V_{222}^{(1)} = \int_0^1 dx dy dz_1 dz_2 dz_3 x y (1-x) (1-y) U^{-2}, \quad (9)$$

$$U = x y (1-x)(1-y) \xi + y (1-x) \chi(z_1; p_2^2; m_1, m_2) \\ + x y \chi(z_2; P^2; m_4, m_3) + x (1-x)(1-y) \chi(z_3; p_1^2; m_5, m_6),$$

$$\xi = - [P^2 (z_2 - z_3) (1 - z_1 - z_2) + p_1^2 (z_2 - z_3) (1 - z_1 - z_3) + p_2^2 (1 - z_1 - z_3) (1 - z_1 - z_2)],$$

$$\chi(z; p^2; m, M) = -p^2 z (1-z) + m^2 (1-z) + M^2 z.$$

Here and in the following we use the short-hand notation

$$\int_0^1 dx dy \cdots dz_3 = \int_0^1 dx \int_0^1 dy \cdots \int_0^1 dz_3.$$

4.1 Non-planar diagram: two internal fermions

In Fig. 3(a) the following mass configuration of the V_{222} -family appears,

$$m_1 = m_5 = 0, \quad m_2 = m_e, \quad m_3 = m_4 = m_6 = M_W, \quad P^2 = M_Z^2, \quad p_1^2 = p_2^2 = m_e^2. \quad (10)$$

The divergence comes entirely from the fermion-photon interaction, so it is possible to set $p_1^2 = 0$. Inserting these values into (9) the resulting expression for the scalar integral $V_{222}^{(1)}$ reads

$$V_{222}^{(1)} = \int_0^1 dy dz_1 dz_2 dz_3 y (1-y) I, \quad \text{with} \quad I = \int_0^1 dx \frac{x(1-x)}{[x(ax+b) + m_e^2 c(x)]^2}, \quad (11)$$

where a , b and $c(x)$ depend on M_W , P^2 , and on the Feynman-parameters y , z_1 , z_2 , and z_3 . In particular, b is linear in z_1 and z_3 ,

$$\begin{aligned} b &= \alpha z_1 z_3 + \beta z_1 + \gamma z_3 + \delta, & \text{with} \\ \alpha &= M_Z^2 y (1-y), \\ \beta &= -M_Z^2 y (1-y) z_2, \\ \gamma &= (1-y)[M_W^2 - M_Z^2 y (1-z_2)], \\ \delta &= y [M_W^2 - M_Z^2 y z_2 (1-z_2)]. \end{aligned} \quad (12)$$

Moreover, the following relations hold,

$$c(0) = y z_1^2, \quad a + b = y [M_W^2 - M_Z^2 z_2(1 - z_2)]. \quad (13)$$

From (11) one can see that, for $m_e = 0$, I is divergent at $x = 0$. The divergence can be extracted as $\ln m_e^2$ in the following way:

$$I = I_a + I_b = \int_0^1 dx \left\{ \left[\frac{x(1-x)}{[x(ax+b) + m_e^2 c(x)]^2} - \frac{x}{[xb + m_e^2 c(0)]^2} \right] + \frac{x}{[xb + m_e^2 c(0)]^2} \right\}. \quad (14)$$

I_a is not divergent and we are free to set $m_e = 0$,

$$I_a = \int_0^1 dx \frac{1}{x} \left[\frac{1-x}{(ax+b)^2} - \frac{1}{b^2} \right] = -\frac{1}{b^2} \left(\ln \frac{a+b}{b} + 1 \right). \quad (15)$$

In I_b , the divergence can be extracted by integrating in x ,

$$I_b = -\frac{1}{b^2} \left[\ln m_e^2 + \ln c(0) - \ln b + 1 \right]. \quad (16)$$

Thanks to the linearity of b with respect to z_1 and z_3 , we can now perform the z_1, z_3 integrations explicitly. Taking into account (12) and (13), the following types of integrals remain:

$$\begin{aligned} \int_0^1 dz_1 dz_3 \frac{1}{b^2} &= \int_0^1 \frac{dz_1 dz_3}{(\alpha z_1 z_3 + \beta z_1 + \gamma z_3 + \delta)^2} = \frac{1}{d} \ln \left(1 + \frac{d}{[\beta\delta][\gamma\delta]} \right), \\ \int_0^1 dz_1 dz_3 \frac{\ln z_1}{b^2} &= \frac{1}{d} \left\{ \text{Li}_2 \left(-\frac{[\alpha\beta]}{[\gamma\delta]} \right) - \text{Li}_2 \left(-\frac{\beta}{\delta} \right) \right\}, \\ \int_0^1 dz_1 dz_3 \frac{\ln b - 1}{b^2} &= \frac{1}{d} \left\{ \text{Li}_2 \left(\frac{d}{\alpha[\alpha\beta\gamma\delta]} \right) - \text{Li}_2 \left(\frac{d}{\alpha[\beta\delta]} \right) - \text{Li}_2 \left(\frac{d}{\alpha[\gamma\delta]} \right) + \text{Li}_2 \left(\frac{d}{\alpha\delta} \right) \right. \\ &\quad - \ln[\alpha\beta\gamma\delta] \ln \left(1 - \frac{d}{\alpha[\alpha\beta\gamma\delta]} \right) + \ln[\beta\delta] \ln \left(1 - \frac{d}{\alpha[\beta\delta]} \right) \\ &\quad \left. + \ln[\gamma\delta] \ln \left(1 - \frac{d}{\alpha[\gamma\delta]} \right) - \ln \delta \ln \left(1 - \frac{d}{\alpha\delta} \right) \right\}, \quad (17) \end{aligned}$$

where we have introduced $d = \alpha\delta - \beta\gamma$ and $[\alpha_1 \dots \alpha_n] = \alpha_1 + \dots + \alpha_n$. It is important to note that the only denominator appearing in the result (d) is now multiplied by "regulator functions" which vanish when d goes to 0. The result is therefore smooth enough to be directly inserted into (11), and the remaining z_2, y integrations are done numerically.

The computation of the tensor integrals $V_{222}^{(\mu, \mu\nu, \mu\nu\rho)}$ is processed in the same way. The new feature is the presence of z_3 to some power $m > 0$ in the integrand. The previous formulae are now replaced by the following ones, where an integration by parts in z_3 is performed:

$$\int_0^1 dz_1 dz_3 \frac{z_3^m}{b^2} = \int_0^1 dz_3 \frac{m z_3^{m-1}}{d} \ln \left(1 + \frac{(1-z_3) d}{[\gamma\delta]([\alpha\gamma]z_3 + [\beta\delta])} \right),$$

$$\int_0^1 dz_1 dz_3 z_3^m \frac{\ln z_1}{b^2} = \int_0^1 dz_3 \frac{m z_3^{m-1}}{d} \left\{ \text{Li}_2 \left(-\frac{[\alpha\beta]}{[\gamma\delta]} \right) - \text{Li}_2 \left(-\frac{\alpha z_3 + \beta}{\gamma z_3 + \delta} \right) \right\},$$

$$\begin{aligned} \int_0^1 dz_1 dz_3 z_3^m \frac{(\ln b - 1)}{b^2} &= \int_0^1 dz_3 \frac{m z_3^{m-1}}{d} \left\{ \text{Li}_2 \left(\frac{d}{\alpha[\alpha\beta\gamma\delta]} \right) - \text{Li}_2 \left(\frac{d}{\alpha([\alpha\gamma]z_3 + [\beta\delta])} \right) \right. \\ &\quad - \text{Li}_2 \left(\frac{d}{\alpha[\gamma\delta]} \right) + \text{Li}_2 \left(\frac{d}{\alpha(\gamma z_3 + \delta)} \right) - \ln[\alpha\beta\gamma\delta] \ln \left(1 - \frac{d}{\alpha[\alpha\beta\gamma\delta]} \right) \\ &\quad + \ln([\alpha\gamma]z_3 + [\beta\delta]) \ln \left(1 - \frac{d}{\alpha([\alpha\gamma]z_3 + [\beta\delta])} \right) \\ &\quad \left. + \ln[\gamma\delta] \ln \left(1 - \frac{d}{\alpha[\gamma\delta]} \right) - \ln(\gamma z_3 + \delta) \ln \left(1 - \frac{d}{\alpha(\gamma z_3 + \delta)} \right) \right\}. \quad (18) \end{aligned}$$

4.2 Non-planar diagram: four internal fermions

Fig. 3(b) corresponds to the configuration

$$m_1 = 0, \quad m_2 = m_3 = m_4 = m_6 = m_e, \quad m_5 = M_Z \quad P^2 = M_Z^2, \quad p_1^2 = p_2^2 = m_e^2. \quad (19)$$

This is an example for a diagram with a double collinear divergence. In order to regularize these divergences the masses of all internal electrons are kept and $p_1^2 = m_e^2 = p_2^2$ is used. In the following the scalar integral $V_{222}^{(1)}$ is considered; the tensor integrals can be calculated as in section 4.1 .

We apply the same parametrization as in section 4.1 and change parameters according to $z_{2,3} \rightarrow 1 - z_{2,3}$, $z_1 \leftrightarrow z_3$. The following expression is obtained,

$$V_{222}^{(1)} = \int_0^1 dy dz_3 y (1-y) J, \quad \text{with} \quad J = \int_0^1 dx dz_1 dz_2 \frac{x(1-x)}{(\rho + m_e^2 \sigma - i\delta)^2}, \quad (20)$$

$$\begin{aligned} \rho &= -x \left\{ y z_2 (1-z_2) - (1-x)(1-y)[z_1 + y(z_1 - z_2)(z_2 - z_3)] \right\} M_Z^2, \\ \sigma &= -x y (1-x)(1-y)(z_1 - z_3)^2 + (1-x) y z_3^2 + x y + x(1-x)(1-y)(1-z_1)^2. \end{aligned}$$

Since ρ is of the type $\rho = x(z_1 A + z_2 B + z_1 z_2 C)$, one can easily see from eq.(20) that, for $m_e = 0$, $V_{222}^{(1)}$ diverges at $x = 0$ and at $z_1 = 0 = z_2$. J can be calculated in the following way:

$$J = J_a + J_b + J_c + J_d = [J - J_x - J_z + J_{xz}] + [J_x - J_{xz}] + [J_z - J_{xz}] + J_{xz}, \quad (21)$$

$$\begin{aligned}
J_x &= \int_0^1 dx dz_1 dz_2 \frac{x(1-x)}{(\rho + m_e^2 \sigma)^2} \Big|_{x^2=x m_e^2=0}, & J_z &= \int_0^1 dx dz_1 dz_2 \frac{x(1-x)}{(\rho + m_e^2 \sigma)^2} \Big|_{\substack{z_1^2=z_2^2=z_1 z_2=0 \\ z_1 m_e^2=z_2 m_e^2=0}}, \\
J_{xz} &= \int_0^1 dx dz_1 dz_2 \frac{x(1-x)}{(\rho + m_e^2 \sigma)^2} \Big|_{\substack{x^2=z_1^2=z_2^2=z_1 z_2=0 \\ x m_e^2=z_1 m_e^2=z_2 m_e^2=0}}.
\end{aligned}$$

J_a is finite for $m_e = 0$, while J_b and J_c involve a single divergence (at $x = 0$ and $z_1 = 0 = z_2$, respectively), giving raise to a simple logarithm in m_e^2 . Finally, J_d contains the double divergence at $x = 0$ and $z_1 = 0 = z_2$, and we extract also a $\ln^2 m_e^2$ term accordingly. Now we define:

$$\begin{aligned}
a + b &= -y z_2 (1 - z_2) M_Z^2 - i\delta, \\
b &= \{(1-y)[z_1 + y(z_1 - z_2)(z_2 - z_3)] - y z_2 (1 - z_2)\} M_Z^2 - i\delta, \\
a_0 + b_0 &= -y z_2 M_Z^2 - i\delta, \\
b_0 &= \{(1-y)[z_1 - y z_3 (z_1 - z_2)] - y z_2\} M_Z^2 - i\delta,
\end{aligned} \tag{22}$$

$$\begin{aligned}
A &= (1-x)(1-y)(1-y z_3) M_Z^2 - i\delta, & B &= -y [1 - (1-x)(1-y) z_3] M_Z^2 - i\delta, \\
A_0 \equiv A|_{x=0} &= (1-y)(1-y z_3) M_Z^2 - i\delta, & B_0 \equiv B|_{x=0} &= -y [1 - (1-y) z_3] M_Z^2 - i\delta,
\end{aligned}$$

$$\begin{aligned}
\sigma_0 &= \sigma|_{z_1=z_2=0} = [1 - x(1-y)] [x + (1-x)y z_3^2], \\
\sigma_{00} &= \sigma|_{x=0} = \sigma|_{x=z_1=z_2=0} = y z_3^2.
\end{aligned}$$

With these notations we obtain for J_a , setting $m_e = 0$,

$$\begin{aligned}
J_a &= \int_0^1 dx dz_1 dz_2 \frac{1}{x} \left[\frac{1-x}{(ax+b)^2} - \frac{1}{b^2} - \frac{1-x}{(a_0x+b_0)^2} + \frac{1}{b_0^2} \right] \\
&= \int_0^1 dz_1 dz_2 \left[\frac{\ln b - \ln(a+b) - 1}{b^2} - \frac{\ln b_0 - \ln(a_0+b_0) - 1}{b_0^2} \right].
\end{aligned} \tag{23}$$

The resulting expressions are of the form (17) and can be integrated in z_1 and z_3 accordingly. Since in this case both γ , δ and d of (17) factorize a z_2 , we get a factor $1/z_2$, that is not multiplied by regulator functions. However, even if the integrals containing $1/b^2$ and $1/b_0^2$ are separately divergent, the combination of the two is finite, because they have the same behaviour around $z_2 = 0$. Therefore, after applying (17), the contribution from J_a to $V_{222}^{(1)}$ can be safely integrated numerically.

For J_b we proceed in an analogous way integrating in x , and obtain

$$\begin{aligned}
J_b &= \int_0^1 dx dz_1 dz_2 \left[\frac{x}{(xb + m_e^2 \sigma_{00})^2} - \frac{x}{(xb_0 + m_e^2 \sigma_{00})^2} \right] \\
&= \int_0^1 dz_1 dz_2 \left[\frac{\ln b - \ln \sigma_{00} - 1}{b^2} - \frac{\ln b_0 - \ln \sigma_{00} - 1}{b_0^2} - \ln(m_e^2) \left(\frac{1}{b^2} - \frac{1}{b_0^2} \right) \right].
\end{aligned} \tag{24}$$

Again, these terms are of the same form as in the expression for J_a and can be integrated analytically in z_1 and z_3 and then numerically in y and z_2 .

To extract the logarithmic behaviour for J_c we have to integrate in z_1 and z_2 , yielding

$$\begin{aligned}
J_c &= \int_0^1 dx dz_1 dz_2 \left\{ \frac{x(1-x)}{[x(Az_1 + Bz_2) + m_e^2 \sigma_0]^2} - \frac{x}{[x(A_0 z_1 + B_0 z_2) + m_e^2 \sigma_{00}]^2} \right\} \\
&= - \int_0^1 dx \frac{1}{x} \left[\frac{(1-x)[\ln(A+B) - \ln A - \ln B - \ln x + \ln \sigma_0]}{AB} \right. \\
&\quad \left. - \frac{\ln(A_0+B_0) - \ln A_0 - \ln B_0 - \ln x + \ln \sigma_{00}}{A_0 B_0} + \ln(m_e^2) \left(\frac{1-x}{AB} - \frac{1}{A_0 B_0} \right) \right]. \quad (25)
\end{aligned}$$

The factors y , $(1-y)$, and $(1-x)$ in the denominators of this expression are always cancelled by those present in the numerator. The overall factor $1/x$ is again regularized by the difference between the terms with A, B, σ_0 and those with A_0, B_0, σ_{00} . The remaining y and z_3 integrations can be done numerically.

Finally, for J_d we integrate in x, z_1 and z_2 , yielding

$$\begin{aligned}
J_d &= \int_0^1 dx dz_1 dz_2 \frac{x}{[x(A_0 z_1 + B_0 z_2) + m_e^2 \sigma_{00}]^2} \\
&= \frac{1}{A_0 B_0} \left[\text{Li}_2 \left(-\frac{A_0 + B_0}{m_e^2 \sigma_{00}} \right) - \text{Li}_2 \left(-\frac{A_0}{m_e^2 \sigma_{00}} \right) - \text{Li}_2 \left(-\frac{B_0}{m_e^2 \sigma_{00}} \right) \right]. \quad (26)
\end{aligned}$$

The dilogarithms can be expanded according to

$$\text{Li}_2 \left(-\frac{c}{m_e^2} \right) = -\frac{\pi^2}{6} - \frac{1}{2} (\ln c - \ln m_e^2)^2 + \mathcal{O}(m_e^2), \quad (27)$$

giving rise to a term proportional to $\ln^2 m_e^2$. The resulting expression is suitable for numerical integration.

5 Results

In Tab. 1 the set of input parameters for our numerical evaluation is listed. M_W and M_Z are the experimental values of the W - and Z -boson masses, which are the on-shell masses. They have to be converted to the values in the pole mass scheme [7], labeled as \overline{M}_W and \overline{M}_Z , which are used internally for the calculation. These quantities are related via $M_{W,Z} = \overline{M}_{W,Z} + \Gamma_{W,Z}^2 / (2 M_{W,Z})$. For Γ_Z the experimental value (Tab. 1) and for Γ_W the theoretical value has been used, *i.e.* $\Gamma_W = 3 G_\mu M_W^3 / (2\sqrt{2}\pi) (1 + 2\alpha_s(M_W^2) / (3\pi))$ with sufficient accuracy.

Our results in terms of $\Delta\kappa$ for the bosonic contributions are shown in Tab. 2, in comparison with the fermionic ones. The last two columns of Tab. 2 contain the corresponding results from [15], which agree with ours.

parameter	value
M_W	80.404 GeV
M_Z	91.1876 GeV
Γ_Z	2.4952 GeV
m_t	172.5 GeV
$\Delta\alpha(M_Z^2)$	0.05907
$\alpha_s(M_Z^2)$	0.119
$\frac{G_\mu}{\overline{M}_W}$	1.16637×10^{-5}
\overline{M}_W	80.3766 GeV
\overline{M}_Z	91.1535 GeV

Table 1: Input parameters. M_W and M_Z are the experimental values for the W - and Z -boson mass, whereas \overline{M}_W and \overline{M}_Z are calculated quantities in the pole mass scheme.

M_H [GeV]	$\Delta\kappa_{\text{ferm}}^{(\alpha^2)} \times 10^{-4}$	$\Delta\kappa_{\text{bos}}^{(\alpha^2)} \times 10^{-4}$	$\Delta\kappa_{\text{ferm}}^{(\alpha^2)} \times 10^{-4}$ [15]	$\Delta\kappa_{\text{bos}}^{(\alpha^2)} \times 10^{-4}$ [15]
100	1.07	-0.74	1.07	-0.74
200	-0.33	-0.47	-0.32	-0.47
600	-2.89	0.18	-2.89	0.17
1000	-2.62	1.11	-2.61	1.11

Table 2: Bosonic two-loop corrections to $\Delta\kappa$ in comparison with the fermionic ones, and the results from [15].

One can see from Tab. 2 that the bosonic corrections are basically of the same order of magnitude as the fermionic ones, as long as the W -mass is taken as a fixed input parameter. The situation changes, however, when instead of the W -mass the Fermi constant is taken as an input parameter and M_W is derived via (3). In order to identify the various sources of the two-loop contributions to $\sin^2\theta_{\text{eff}}$, we expand both quantities M_W and κ according to $\{M_W, \kappa\} = \{M_W, \kappa\}^{(\text{tree}+\alpha)} + \{M_W, \kappa\}^{(\alpha^2)} + \mathcal{O}(\alpha^3)$, yielding

$$\begin{aligned}
\sin^2\theta_{\text{eff}} &= \sin^2\theta_{\text{eff}}^{(\text{tree}+\alpha)} + \Delta\sin^2\theta_{\text{eff}}(\Delta M_W^{(\alpha^2)}) + \Delta\sin^2\theta_{\text{eff}}(\Delta\kappa^{(\alpha^2)}) + \mathcal{O}(\alpha^3) \\
&= \left(1 - \frac{(M_W^{(\text{tree}+\alpha)})^2}{M_Z^2}\right) \kappa^{(\text{tree}+\alpha)} - 2\frac{m_W}{m_Z^2} \Delta M_W^{(\alpha^2)} + \left(1 - \frac{m_W^2}{m_Z^2}\right) \Delta\kappa^{(\alpha^2)} + \mathcal{O}(\alpha^3)
\end{aligned} \tag{28}$$

The first term represents the one-loop result, while the other two terms correspond to the electroweak two-loop contributions to the shift in the W mass, $\Delta M_W^{(\alpha^2)}$, and to the shift in κ , $\Delta\kappa^{(\alpha^2)}$. As can be seen in Tab. 3, the fermionic corrections from M_W dominate, while the contributions from M_W and κ in the bosonic sector cancel to a large extent.

In Tab. 4, the results for M_W , as taken from [15], and $\sin^2\theta_{\text{eff}}$ are shown with only the fermionic two-loop corrections (M_W^{ferm} and $\sin^2\theta_{\text{eff}}^{\text{ferm}}$) and with both fermionic and bosonic two-loop corrections ($M_W^{\text{ferm}+\text{bos}}$ and $\sin^2\theta_{\text{eff}}^{\text{ferm}+\text{bos}}$) for various values of M_H . Besides the

M_H	$\Delta \sin^2\theta_{\text{eff}}(\Delta M_{W,\text{ferm}}^{(\alpha^2)})$	$\Delta \sin^2\theta_{\text{eff}}(\Delta k_{\text{ferm}}^{(\alpha^2)})$	$\Delta \sin^2\theta_{\text{eff}}(\Delta M_{W,\text{bos}}^{(\alpha^2)})$	$\Delta \sin^2\theta_{\text{eff}}(\Delta k_{\text{bos}}^{(\alpha^2)})$
100	93.89	2.38	1.93	-1.65
200	98.51	-0.73	0.97	-1.05
600	106.89	-6.43	0.19	0.40
1000	105.36	-5.83	-1.16	2.47

Table 3: Fermionic and bosonic electroweak two-loop corrections to $\sin^2\theta_{\text{eff}}$. M_H is given in GeV; the values for $\Delta \sin^2\theta_{\text{eff}}$ have to be multiplied by 10^{-5} .

M_H [GeV]	M_W^{ferm} [GeV]	$M_W^{\text{ferm+bos}}$ [GeV]	$\sin^2\theta_{\text{eff}}^{\text{ferm}}$	$\sin^2\theta_{\text{eff}}^{\text{ferm+bos}}$	$\sin^2\theta_{\text{eff}}^{\text{bos}} [10^{-4}]$
100	80.3694	80.3684	0.231459	0.231461	0.02
200	80.3276	80.3270	0.231792	0.231792	0
600	80.2491	80.2490	0.232346	0.232352	0.06
1000	80.2134	80.2141	0.232587	0.232599	0.12

Table 4: M_W and $\sin^2\theta_{\text{eff}}$ without (ferm) and with (ferm+bos) bosonic two-loop corrections. $\sin^2\theta_{\text{eff}}^{\text{bos}}$ is the purely bosonic contribution to $\sin^2\theta_{\text{eff}}$.

electroweak one- and two-loop corrections, the results for $\sin^2\theta_{\text{eff}}$ also contain the QCD-corrections of order $\mathcal{O}(\alpha\alpha_s)$ and $\mathcal{O}(\alpha\alpha_s^2)$ [6], as well as the leading three-loop corrections of order $\mathcal{O}(\alpha^2\alpha_s m_t^4)$ and $\mathcal{O}(\alpha^3 m_t^6)$ [9].

The shifts in $\sin^2\theta_{\text{eff}}$ originating from the full set of bosonic two-loop contributions are displayed in the last column of Tab. 4. According to the cancellations mentioned above, they are much smaller than the corresponding shifts for a fixed value of the W mass as an input parameter, which would result from eq. (2) with the values of $\Delta\kappa$ given in Tab. 2.

6 Conclusion

In conclusion, we have completed the calculation of the electroweak bosonic two-loop corrections to the effective leptonic mixing angle $\sin^2\theta_{\text{eff}}$. A comparison of our results with the ones in [15] was performed and full agreement was found. The bosonic corrections are basically of the same order of magnitude as the fermionic ones when the W -mass is taken as a fixed input parameter. If instead the Fermi constant is taken as input, with M_W as a derived quantity, the bosonic corrections to $\sin^2\theta_{\text{eff}}$ are quite small.

In addition, the use of the general techniques of [22] to treat IR-divergences provides a good test of their applicability to physical processes. In particular we have shown that in this approach the cancellation of the infrared poles can be verified analytically. Moreover, our complete calculation of the two-loop electroweak corrections of $\sin^2\theta_{\text{eff}}$ is the first physical application of the numerical methods of [21] showing that these methods are

really applicable in practice for the calculation of physical quantities. In particular within this approach massive two-loop vertices with many mass scales are computed “directly”, so not using mass expansions, which could represent a good way to deal also with calculations beyond the Standard Model, where often many (unknown) massive particles come into the game.

Acknowledgement

W.H. is grateful to the Institute of Theoretical Physics, University of Vienna, where this paper was finalized while he was Erwin Schrödinger visiting professor.

References

- [1] The LEP Collaborations, the LEP Electroweak Working Group, the SLD Electroweak and Heavy Flavour Groups, *Phys. Rep.* **427** (2006) 257 [arXiv:hep-ex/0509008]. D. Wood, XXIII International Conference on High Energy Physics, Moscow 2006.
- [2] J. A. Aguilar-Saavedra *et al.*, TESLA Technical Design Report Part III: *Physics at an e^+e^- Linear Collider* [hep-ph/0106315]. T. Abe *et al.* [American Linear Collider Working Group Collaboration], in *Proc. of the APS/DPF/DPB Summer Study on the Future of Particle Physics (Snowmass 2001)* ed. R. Davidson and C. Quigg, SLAC-R-570, *Resource book for Snowmass 2001* [hep-ex/0106055, hep-ex/0106056, hep-ex/0106057, hep-ex/0106058]. K. Abe *et al.* [ACFA Linear Collider Working Group Collaboration], ACFA Linear Collider Working Group report, [hep-ph/0109166].
- [3] U. Baur, R. Clare, J. Erler, S. Heinemeyer, D. Wackerroth, G. Weiglein and D. R. Wood, in *Proc. of the APS/DPF/DPB Summer Study on the Future of Particle Physics (Snowmass 2001)* ed. N. Graf, eConf **C010630** (2001) P122 [arXiv:hep-ph/0111314].
- [4] D. Y. Bardin *et al.*, arXiv:hep-ph/9709229, in *Precision Calculations for the Z Resonance*, D. Bardin, W. Hollik, G. Passarino (Eds.), CERN 95-03.
- [5] A. Djouadi and C. Verzegnassi, *Phys. Lett. B* **195** (1987) 265; A. Djouadi, *Nuovo Cim. A* **100** (1988) 357; B. A. Kniehl, *Nucl. Phys. B* **347** (1990) 86; F. Halzen and B. A. Kniehl, *Nucl. Phys. B* **353** (1991) 567; B. A. Kniehl and A. Sirlin, *Nucl. Phys. B* **371** (1992) 141; A. Djouadi and P. Gambino, *Phys. Rev. D* **49** (1994) 3499 [Erratum-ibid. *D* **53** (1996) 4111] [arXiv:hep-ph/9309298].
- [6] K. G. Chetyrkin, J. H. Kühn and M. Steinhauser, *Phys. Rev. Lett.* **75** (1995) 3394 [arXiv:hep-ph/9504413], *Nucl. Phys. B* **482** (1996) 213 [arXiv:hep-ph/9606230].

- [7] A. Freitas, W. Hollik, W. Walter and G. Weiglein, Phys. Lett. B **495** (2000) 338, E: ibid. B **570** (2003) 260 [arXiv:hep-ph/0007091] and Nucl. Phys. B **632** (2002) 189, E: ibid. B **666** (2003) 305 [arXiv:hep-ph/0202131]. M. Awramik and M. Czakon, Phys. Lett. B **568**, 48 (2003) [arXiv:hep-ph/0305248].
- [8] M. Awramik and M. Czakon, Phys. Rev. Lett. **89** (2002) 241801 [arXiv:hep-ph/0208113]. A. Onishchenko and O. Veretin, Phys. Lett. B **551** (2003) 111 [arXiv:hep-ph/0209010]. M. Awramik, M. Czakon, A. Onishchenko and O. Veretin, Phys. Rev. D **68**, 053004 (2003) [arXiv:hep-ph/0209084].
- [9] J. van der Bij, K. Chetyrkin, M. Faisst, G. Jikia and T. Seidensticker, Phys. Lett. B **498** (2001) 156 [arXiv:hep-ph/0011373]. M. Faisst, J. H. Kühn, T. Seidensticker and O. Veretin, Nucl. Phys. B **665**, 649 (2003) [arXiv:hep-ph/0302275].
- [10] R. Boughezal, J.B. Tausk and J.J. van der Bij, Nucl. Phys. B **713**, 278 (2005) [arXiv:hep-ph/0410216]. Y. Schroder and M. Steinhauser, Phys. Lett. B **622** (2005) 124 [arXiv:hep-ph/0504055]. K. G. Chetyrkin, M. Faisst, J. H. Kuhn, P. Maierhofer and C. Sturm, arXiv:hep-ph/0605201. R. Boughezal and M. Czakon, arXiv:hep-ph/0606232.
- [11] R. Boughezal, J. B. Tausk and J. J. van der Bij, Nucl. Phys. B **725** (2005) 3 [arXiv:hep-ph/0504092].
- [12] M. Awramik, M. Czakon, A. Freitas and G. Weiglein, Phys. Rev. Lett. **93** (2004) 201805 [arXiv:hep-ph/0407317]; Nucl. Phys. Proc. Suppl. **135** (2004) 119 [arXiv:hep-ph/0408207].
- [13] W. Hollik, U. Meier and S. Uccirati, Nucl. Phys. B **731** (2005) 213 [arXiv:hep-ph/0507158].
- [14] W. Hollik, U. Meier and S. Uccirati, Phys. Lett. B **632** (2006) 680 [arXiv:hep-ph/0509302].
- [15] M. Awramik, M. Czakon and A. Freitas, arXiv:hep-ph/0605339; arXiv:hep-ph/0608099.
- [16] J. Küblbeck, M. Böhm and A. Denner, Comp. Phys. Comm. **60** (1990) 165. T. Hahn, Nucl. Phys. Proc. Suppl. **89** (2000) 231 [arXiv:hep-ph/0005029], Comput. Phys. Commun. **140** (2001) 418 [arXiv:hep-ph/0012260], *FeynArts User's Guide*, available at <http://www.feynarts.de>.
- [17] G. Weiglein, R. Scharf and M. Böhm, Nucl. Phys. B **416** (1994) 606 [arXiv:hep-ph/9310358]; G. Weiglein, R. Mertig, R. Scharf and M. Böhm, PRINT-95-128 *Prepared for 2nd International Workshop on Software Engineering, Artificial Intelligence and Expert Systems for High-energy and Nuclear Physics, La Londe Les Maures, France, 13-18 Jan 1992*

- [18] G. 't Hooft and M. J. G. Veltman, Nucl. Phys. B **153** (1979) 365.
- [19] A. I. Davydychev and J. B. Tausk, Nucl. Phys. B **397** (1993) 123.
- [20] S. Bauberger, M. Böhm, G. Weiglein, F. A. Berends and M. Buza, Nucl. Phys. Proc. Suppl. **37B** (1994) 95 [arXiv:hep-ph/9406404]; S. Bauberger, F. A. Berends, M. Böhm and M. Buza, Nucl. Phys. B **434** (1995) 383 [arXiv:hep-ph/9409388]; S. Bauberger and M. Böhm, Nucl. Phys. B **445** (1995) 25 [arXiv:hep-ph/9501201].
- [21] A. Ferroglia, M. Passera, G. Passarino and S. Uccirati, Nucl. Phys. B **680** (2004) 199 [arXiv:hep-ph/0311186] and Nucl. Phys. B **650** (2003) 162 [arXiv:hep-ph/0209219]; S. Actis, A. Ferroglia, G. Passarino, M. Passera and S. Uccirati, Nucl. Phys. B **703** (2004) 3 [arXiv:hep-ph/0402132]; G. Passarino, Nucl. Phys. B **619** (2001) 257 [arXiv:hep-ph/0108252]; G. Passarino and S. Uccirati, Nucl. Phys. B **629** (2002) 97 [arXiv:hep-ph/0112004]; S. Uccirati, Acta Phys. Polon. B **35** (2004) 2573 [arXiv:hep-ph/0410332].
- [22] G. Passarino and S. Uccirati, Nucl. Phys. B **747** (2006) 113 [arXiv:hep-ph/0603121].